International Journal of Applied Earth Observations and Geoinformation 107 (2022) 102684

Contents lists available at ScienceDirect

International Journal of Applied Earth Observations and Geoinformation

journal homepage: www.elsevier.com/locate/jag

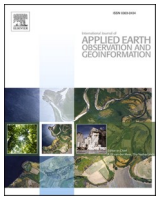

An intensity-enhanced method for handling mobile laser scanning point clouds

Lina Fang [a,b], Hao Chen [a,b], Huan Luo [a,c,d,*], Yingya Guo [c,d], Jonathon Li [e]

[a] Key Laboratory of Spatial Data Mining and Information Sharing of MOE, Fuzhou University, FJ 350116, China
[b] Academy of Digital China (Fujian), Fuzhou University, Fuzhou, FJ 350116, China
[c] Fujian Provincial Key Laboratory of Network Computing and Intelligent Information Processing, Fuzhou University, Fuzhou, FJ 350116, China
[d] College of Computer Science and Big Data, Fuzhou University, Fuzhou, FJ 350116, China
[e] Department of Geography and Environmental Management and Department of Systems Design Engineering, University of Waterloo, Waterloo, ON N2L 3G1, Canada

ARTICLE INFO

Keywords:
Point Cloud
Intensity Enhancement
Point Cloud Denoising
Dark Channel Prior
Mobile Laser Scanning

ABSTRACT

Currently, mobile laser scanning (MLS) systems can conveniently and rapidly measure the backscattered laser beam properties of the object surfaces in large-scale roadway scenes. Such properties is digitalized as the intensity value stored in the acquired point cloud data, and the intensity as an important information source has been widely used in a variety of applications, including road marking inventory, manhole cover detection, and pavement inspection. However, the collected intensity is often deviated from the object reflectance due to two main factors, i.e. different scanning distances and worn-out surfaces. Therefore, in this paper, we present a new intensity-enhanced method to gradually and efficiently achieve the intensity enhancement in the MLS point clouds. Concretely, to eliminate the intensity inconsistency caused by different scanning distances, the direct relationship between scanning distance and intensity value is modeled to correct the inconsistent intensity. To handle the low contrast between 3D points with different intensities, we proposed to introduce and adapt the dark channel prior for adaptively transforming the intensity information in point cloud scenes. To remove the isolated intensity noises, multiple filters are integrated to achieve the denoising in the regions with different point densities. The evaluations of our proposed method are conducted on four MLS datasets, which are acquired at different road scenarios with different MLS systems. Extensive experiments and discussions demonstrate that the proposed method can exhibit the remarkable performance on enhancing the intensities in MLS point clouds.

1. Introduction

The intelligent technologies on automatically extracting the accurate road information are significant to facilitate the development of urban digital twins or smart cities (Luo et al., 2018; Rastiveis et al., 2020; Mi et al., 2021). Nowadays, Mobile Laser Scanning (MLS) systems equipped with survey-grade laser scanners can efficiently and rapidly perceive the surrounding road environment by actively emitting multiple laser beams to produce the point cloud data. The received energy response of laser beam, which is recorded as intensity value in point-cloud data, can be exploited to measure the reflectivity of object surface (Yang et al., 2012; Wen et al., 2019). As an extremely important information source, intensity-related information has been widely used in massive applications of Intelligent Transportation Systems (ITS), e.g. autonomous driving (Luo et al., 2021; Li et al., 2021; Wang et al., 2021; Fang et al., 2021), transportation facility maintenance (Huang et al., 2017; Yu et al., 2020; Mi et al., 2021), and high-definition (HD) maps (Yang et al., 2017; Pan et al., 2019; Ma et al., 2021; Ye et al., 2021).

Although the intensity information plays an essential role in lots of ITS-related applications, the intensities acquired by MLS systems often cannot correctly reflect the real reflectance of the measured objects due to two main factors, i.e. different scanning distances and worn-out surfaces (Dias et al., 2002; Guan et al., 2014). Specifically, longer scanning distance means lower intensity value, which leads to the intensity inconsistency in the objects locating at different scanning distances, although such objects belong to the same category. In addition, road abrasion deteriorates the flatness of the road surface and influences the reflectivity of object surface, which may introduce the salt-and-pepper noise into the intensities in the collected point-cloud scenes. Therefore, this paper mainly focuses on designing an efficient method to

* Corresponding author.
E-mail address: hluo@fzu.edu.cn (H. Luo).

https://doi.org/10.1016/j.jag.2022.102684
Received 5 November 2021; Received in revised form 22 December 2021; Accepted 10 January 2022
Available online 28 January 2022

correct the intensity values for achieving the intensity enhancement in the MLS point clouds.

To mitigate the obtained intensities that deviate from the reflectivity of real objects, many researchers have attempted to solve the problem on two aspects: i.e. intensity correction (Fang et al., 2015; Wu et al., 2021) and intensity denoising (Schmitz et al., 2019). On one hand, previous studies on intensity correction in point-cloud scenes are either data-driven (Cheng et al., 2017) or model-driven (Ding et al., 2013). Those methods mainly focus on building a mathematical model to describe the direct mapping relationship between the intensity values and different influencing factors. Although these methods have successfully considered the relationship between intensity value and individual factor, they neglect to consider multiple factors into intensity correction like random noise and road surface situation. On the other hand, the past studies on intensity denoising of point clouds were focused on introducing the technologies successfully used in image denoising (Cheng et al., 2021). However, those studies often focus on suppressing intensity noise in the scenario with constant point density but ignore the scenario with different point densities.

In the collected intensity of point-cloud scenes, road abrasion often brings a large number of salt-and-pepper noises, which largely decrease the contrast of points with different intensities. It is observed that such salt-and-pepper noises in the point clouds are similar to the haze in images. To achieve the removal of the haze in a single image, He et al. (2010) integrated the haze imaging model with dark channel prior for the recovery of a no-haze image. Dark channel prior originates from the observation that local patches in the haze-free images often have some pixels with low intensity in at least one color channel (He et al., 2010). By removing the estimated haze from the hazy images under the dark channel prior, the visibility of the images and the low-contrast color shift can be largely improved. Therefore, the dark channel prior can be naturally introduced into achieving a high contrast in the points with different intensities.

In order to achieve the intensity enhancement in MLS point clouds to benefit these intensity-based applications, this paper mainly focuses on proposing an efficient method to correct, transform and denoise intensity by considering different influencing factors. Concretely, to rectify the intensity inconsistency caused by different scanning distances, the relationship between scanning distance and intensity value is modeled to correct the inconsistent intensity. To handle the low contrast between low-intensity and high-intensity points, we introduce the dark channel prior for obtaining a high contrast by transforming the intensity information. To accomplish the removal of the isolated intensity noises, different filters are integrated to achieve the denoising procedure in the point-cloud regions with different point density. Therefore, the main contributions of our paper are summarized as follows:

(1) We propose a new method to achieve the intensity enhancement in MLS point clouds by considering different factors, i.e. the scanning distance, the point density, road abrasion. For each factor, an effective operation is proposed to enhance the intensity for the benefits of those intensity-based applications.
(2) To achieve the high contrast between 3D points with different intensities, we propose to introduce the dark channel prior, which have gained popularity in image defogging, to transform the intensity values. To adapt the dark channel prior to the task of intensity transformation in different point-cloud scenarios, we redesign the dark channel prior used in dehazed images to self-adaptively obtain the optical transmittance and atmospheric light.
(3) Extensive experiments are conducted on four datasets to evaluate the correctness and robustness of our proposed intensity-enhanced method. These datasets are built on large-scale point clouds, which are collected at different road scenarios by different MLS systems. Additionally, the ablation experiments are conducted to demonstrate the functionality of each component in our proposed method.

We organize the rest of our paper as follows. Section 2 introduces the related researches on intensity enhancement in point clouds in detail. Section 3 expounds the workflow of our proposed intensity-enhanced method. Section 4 presents the extensive experimental results to demonstrate the effectiveness of our proposed method. Section 5 concluds the paper.

2. Related work

To improve the quality of acquired intensities of point clouds, many researchers have focused on developing different technologies for intensity enhancement in point clouds. In this section, we introduce the related works of intensity enhancement on the two aspects, i.e. intensity correction and intensity denoising in point clouds.

2.1. Intensity correction in point clouds

Many previous researches on intensity correction of point-cloud data mainly focused on analyzing the relationship between the measured intensity and the various factors, i.e., temperature (Thundathil et al., 2021), humidity (Anttila et al., 2016), geometric characteristics (Höfle and Pfeifer, 2007; Luo et al., 2019), etc. Once the relationship is determined, the mathematical model is built to implement the task of intensity correction in point clouds. Höfle and Pfeifer (2007) systematically studied the intensity correction of point clouds and classified the related studies of intensity correction into two categories: data-driven methods and model-driven methods. Specifically, the model-driven methods mainly studied the mechanisms of laser scanning systems and attempted to establish the intensity-correction model according to the reflectivity of object surfaces or the laser attenuation during the transmission (Li et al., 2016). The data-driven methods mainly focused on exploring homogeneous data to achieve the model fitting which is used to infer the relationship between intensity values and various factors for intensity correction in point clouds (Fang et al., 2015; Tan and Cheng, 2016). For MLS systems, most methods on intensity correction are data-driven. Teo and Yu (2015) achieved the intensity correction by introducing a cubic polynomial function to fit the mapping relationship between the scanning distance and intensity value in MLS point clouds. To handle the unevenly distributed and strongly fluctuated intensities of road makings in MLS point clouds, Cheng et al. (2017) proposed a scan-angle-based intensity correction algorithm by introducing a function to map the incidence angle to the intensities.

2.2. Intensity denoising in point clouds

The acquired point-cloud data inevitably contains intensity noise because of different factors, i.e. road abrasion, the accuracy of scanning systems, atmospheric environment, etc. These intensity noises largely impose an adverse impact on the performance of the intensity enhancement. To elliminate the adverse impact brought by intensity noises, the researches of intensity denoising in point clouds have been attracting wide attentions (Fang et al., 2015; Song et al., 2021). In the past decades, studies on image denoising have been investigated and made progress (Zhang et al., 2020). Naturally, some on-image filters were introduced and applied to the intensity denoising of point cloud data (Al-Shayea et al., 2020). Specifically, to eliminate the high-frequency intensity noises in point clouds, the median filtering, which is applied in image denoising, is introduced to implement the intensity denoising (Yan et al., 2016). To guarantee the intensity consistency in the homogenous objects, median filtering can effectively suppress the extreme point of the intensity and smooth the intensity of the points by considering the intensities of its neighboring points. The neighboring points were often determined according to the spatial distance in the 3D

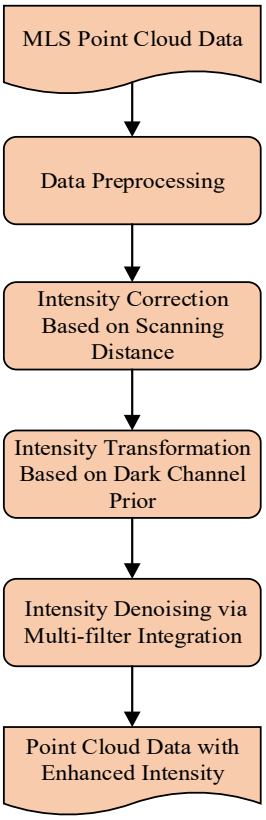

Fig. 1. Flowchart of the proposed method on intensity enhancement in the MLS point clouds.

cooridinate system. However, such neighboring points may not adapt to the scenarios with variations of point densities. Li et al. (2016) proposed a dynamic window median filter to adaptively remove the intensity noises and achieve the intensity enhancement of 3D points in the scanning line way. Although such a median filter can effectively suppress the discretely distributed intensity noise, it cannot achieve the denoising task among the regions with different point densities. Furthermore, the median filter cannot deal with the large area of noises caused by worn-out surface, which commonly occurs in different road scenarios.

Although the studies of intensity correction and intensity denoising in MLS point clouds have gained the significant progress, there is no comprehensive study to solve the problem of intensity enhancement in MLS point clouds by considering multiple factor.

3. Method

The intensity acquired by MLS systems is often affected by various factors including scanning distance, point density, worn-out surface, etc. Our goal is to enhance the collected intensity recorded in point-cloud data by considering such various factors. In this paper, we propose to consider different factors with different models, and combine these models for gradually enhancing the quality of intensity. Fig. 1 presents the workflow of our proposed method on improving the quality of intensity information. As shown in Fig. 1, the input MLS point clouds are first preprocessed by extracting the road points and dividing the road points into segments. Then, we conduct the intensity correction to rectify the intensity inconsistency by exploiting the relationship between the scanning distance and intensity value. After that, in order to enhance the contrast between high-intensity points and low-intensity points, we implement the transformation on intensity values by introducing the dark channel prior. Finally, we remove the points with the isolated noise intensity by integrating multi-filter to handle the regions with different point densities.

3.1. Data preprocessing

To improve the processing efficiency in large-scale point-cloud scenes, necessary data pre-processing is required to implement for extracting the points belonging to the road surface. In this paper, as shown in Fig. 2, we adopt the approaches proposed in (Yang et al., 2013) as the preprocessing steps. Specifically, according to the trajectory points, the whole point clouds collected by the MLS system are first partitioned into a set of consecutive road cross sections. In practice, the length of a cross-section is set at about 25 m. Then, for each road cross section, the road surface points are extracted by applying a moving window operator (Yang et al., 2013). This moving window operator aims to detect the road curb points by finding curb patterns in each scanning line. Once the curb points are detected, the road surface points can be determined.

3.2. Intensity correction based on scanning distance

The objects belong to the same category may have inconsistent intensities because of the different scanning distances (see Fig. 3(a) and 3 (b)). Such intensity inconsistency imposes an negative effect on the performance of intensity-based applications like road markings segmentation (Mahmoudabadi et al., 2016). It is observed that the intensity value is inversely proportional to the scanning distance. But, the distance effect on intensity does not completely follow the inverse range function at a near or large range. The traditional ratio method is easy to cause over-correction at the near or edge range. Considering dynamic platform and instrumental factors of MLS systems, it is hard to finely define the behavior of near range or non-near range according to the distances. Therefore, we use the threshold θ_l instead of the range as the clue to choose the different range correction functions, which describe the relationship between the intensity value and the scanning distance for the elimination of the intensity inconsistency. To assure the intensity consistency, we re-calculate 3D point p's intensity, I_p^r, as follows:

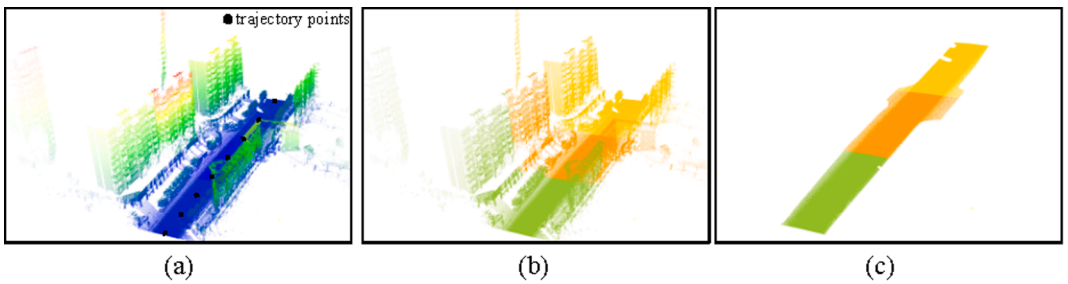

Fig. 2. Illustration on the procedure of data preprocessing in our proposed intensity-enhanced method. (a) is the original point cloud scene acquired by the MLS system. Here, the black points represent the trajectory points; (b) is the partitioned point cloud sections according to the trajectory data; (c) is road surface points obtained by applying the moving windows operator.

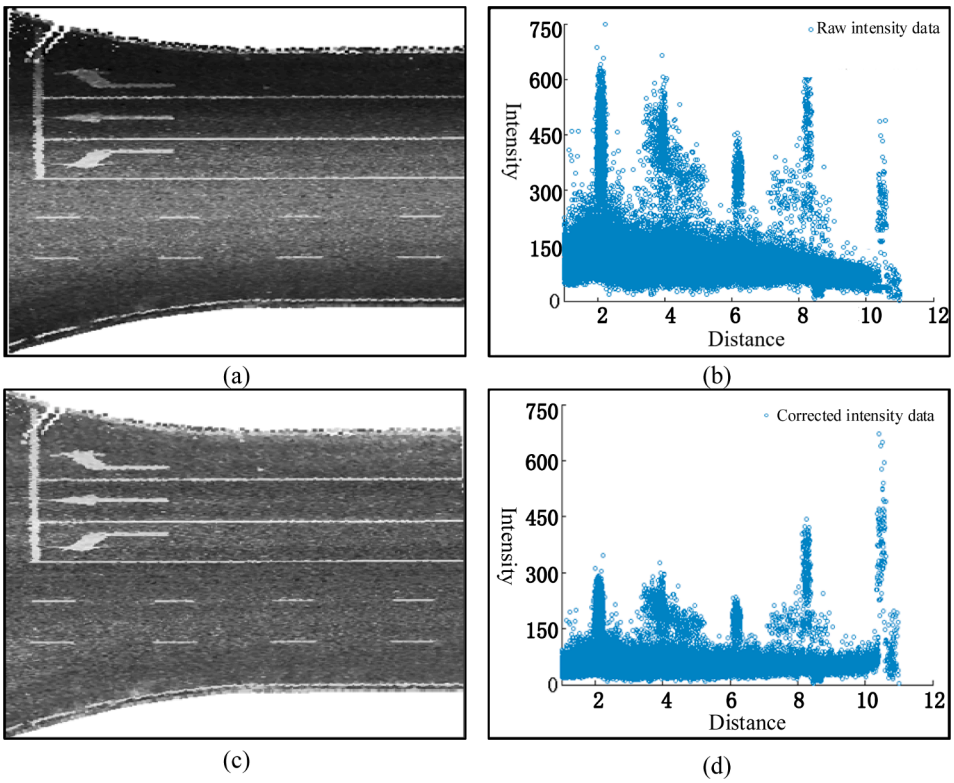

Fig. 3. Example of intensity correction based on scanning distance: (a) original point cloud scene, (b) distribution of scanning distance and intensity value in the original point cloud scene, (c) point cloud scene after intensity correction, and (d) distribution of scanning distance and intensity value after intensity correction.

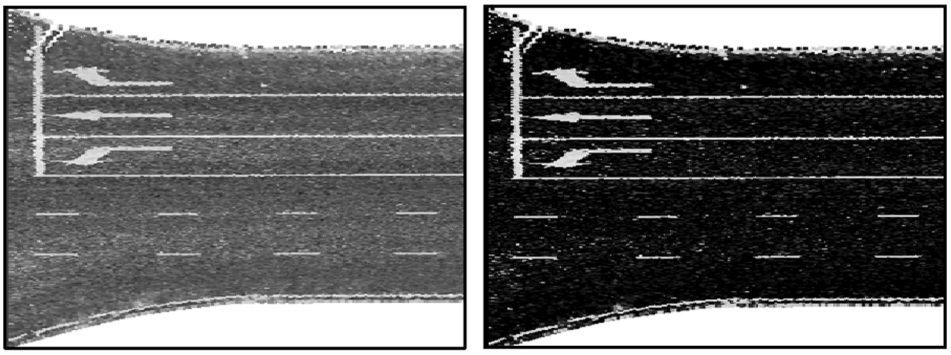

Fig. 4. Illustration of dark channel prior-based intensity transformation: (a) point cloud scene displayed in intensity value after only applying intensity correction, and (b) point cloud scene displayed in intensity value after applying both intensity correction and intensity transformation.

$$I_p^r = \begin{cases} \dfrac{f(\widehat{R})}{f(R_p)} * I_p, \Delta I_p < \theta_I \\ f(\widehat{R}) - f(R_p) + I_p, \Delta I_p \geq \theta_I \end{cases} \tag{1}$$

$$f(R) = \eta_0 + \eta_1 R + \eta_2 R^2 + \eta_3 R^3 \tag{2}$$

$$\Delta I_p = \frac{f(\widehat{R})}{f(R_p)} * I_p - \tag{3}$$

$$\theta_I = \max_{p \in \boldsymbol{P}} \left\{ \frac{I_p}{2} \right\} \tag{4}$$

where I_p is the point p's intensity information collected by the MLS system. $\boldsymbol{P}$ denotes the set of 3D points in the point-cloud segment which is obtained from the data preprocessing. $\widehat{R}$ represents the reference value, which is computed as the minimum spatial distance between points in $\boldsymbol{P}$ and its corresponding trajectory. R_p represents the tridimensional distance between the point p and its corresponding trajectory. Here, we assume that the relationship between intensity and scanning distance is non-linear. Therefore, a cubic polynomial function $f(R)$ is introduced to model the relationship between intensity and scanning distance. The coefficients $\eta_i (i = 0, 1, 2, 3)$ are determined by fitting the homogeneous regions in different scenarios. Concretely, the road surfaces with homogeneous intensities are randomly selected as control patches. Based on these selected control patches, the least square algorithm (Teo and Yu, 2015) is applied to calculate the coefficients in Eq (2). In Eq. (1), when ΔI_p is smaller than the threshold, θ_I, we increase the point p's intensity value exponentially according to the ratio $\frac{f(\widehat{R})}{f(R_p)}$. On the contrary, when ΔI_p is larger than the threshold θ_I, we increase the point p's intensity value linearly according to the difference between $f(\widehat{R})$ and

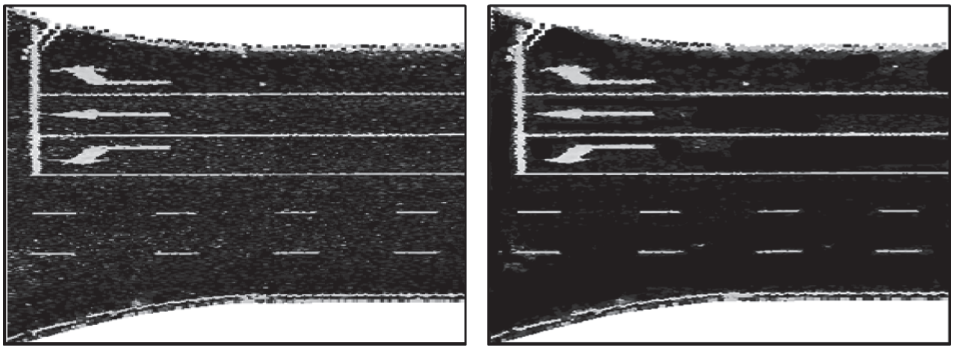

(a) Point clouds with isolated intensity noise (b) Denoised point clouds

Fig. 5. Example of intensity denoising via multi-filter integration in MLS point-cloud scenario.

$f(R_p)$. Here, the threshold, θ_I, is self-adaptively determined on the maximum intensity among the intensities in the corresponding segment by Eq. (4). After rectifying the intensity values by applying Eq. (1), the intensity inconsistency can be effectively removed (see Fig. 3(c) and 3 (d)).

3.3. Intensity transformation based on dark channel prior

Although the intensity inconsistency in collected point clouds can be eliminated by correcting the intensity values based on scanning distances, there is still a large amount of salt-and-pepper intensity noise caused by road abrasion. Such noise influences the intensity values and results in a low contrast among the points with different intensities (see Fig. 4(a)). To remove the influence caused by the salt-and-pepper noise, we introduce the dark channel prior to filter those noise by transforming the intensity values and enlarging the contrast in the points with different intensities (see Fig. 4(b)). The transformed intensities are beneficial to those intensity-based applications.

The dark channel prior proposed by He et al. (2010) has been widely used to remove the haze in a single hazed image. The haze in images causes low brightness and clarity, which makes it difficult to identify object boundaries. Specifically, we treat the point cloud segment with the salt-and-pepper noise as a hazed image. The point-cloud scene, $J(\boldsymbol{P})$, whose intensities have been transformed by dark channel prior, can be obtained as follows:

$$J(\boldsymbol{P}) = \frac{I_r(\boldsymbol{P}) - A}{t(\boldsymbol{P})} + A \tag{5}$$

where $I_r(\boldsymbol{P})$ denotes the intensity values of the point-cloud segment, $\boldsymbol{P}$, which has a lot of the salt-and-pepper noise. A and $t(\boldsymbol{P})$ represent the value of atmospheric light and optical transmittance, respectively. During the procedure of intensity transformation, $t(\boldsymbol{P})$ should be set at a relatively small value. To make Eq. (5) meaningful, we constrain the value of $t(\boldsymbol{P})$ larger than a given minimum value t_0. Therefore, we rewrite Eq. (5) as follows:

$$J(\boldsymbol{P}) = \frac{I_r(\boldsymbol{P}) - A}{\max(t(\boldsymbol{P}), t_0)} + A \tag{6}$$

Here, the atmospheric light A can be calculated as follows:

$$A = \underset{p \in \boldsymbol{P}}{\text{mode}}\{I_r(p)\} \tag{7}$$

In addition, we should consider the intensity noises caused by road abrasion when determining the value of $t(\boldsymbol{P})$. Since pepper noises are associated with high values and wide distribution, we use the histogram statistical method to calculate intensity distribution and estimate the noise information caused by abrasion. Concretely, we divide the range of intensity values in the point cloud segment into $\boldsymbol{M}$ intervals. For each intensity interval $m \in \boldsymbol{M}$, the number of points, n_m, is calculated and the intensity frequency, F_m, can be computed as $n_m/|\boldsymbol{P}|$. Here, $|\boldsymbol{P}|$ gives the total number of points in the point set $\boldsymbol{P}$. Hence, $F_{m_p} * I_r(p)$ can be used to denote the noise characteristics of point p. The transmittance t_p for point, p is derived from the ratio of noise characteristics of each point to the maximum noise characteristic value in its corresponding intensity interval $m_p \in \boldsymbol{M}$ as follows:

$$t_p = \frac{F_{m_p} * I_r(p)}{\max\limits_{m \in \boldsymbol{M}}\{F_m\}} \tag{8}$$

The greater the value of t_p, the more serious noise characteristics. Once the point p's optical transmittance, t_p, is calculated, its transformed intensity,$J(p)$, can be calculated as follows:

$$J(p) = \frac{I_r(p) - A}{\max(t_p, t_0)} + A \tag{9}$$

Through applying the intensity transformation to each point in MLS point clouds according to Eq. (9), the contrast among the points with different densities will be enlarged (see Fig. 4(b)).

3.4. Intensity denoising via Multi-filter integration

After applying the intensity correction and intensity transformation in the MLS point clouds, most of the inaccurate intensity information in the point-cloud segment can be corrected and enhanced. However, there are still some isolated intensity noises caused by measurement errors or the complex surrounding environment (see Fig. 5(a)). To remove those isolated intensity noises, we propose to integrate multiple filters for separately considering the regions with different point densities. Concretely, the distribution of noise points in the high-density region is relatively concentrated, while the isolated noises in the low-density regions are sparsely distributed. Hence, the distribution of noise points makes it difficult to design a model to achieve denoising in regions with different point densities. In our proposed method, we divide the point-cloud segment into two regions, i.e., high-density region and low-density region. Here, a threshold th_c is used to determine whether a region belongs to the high-density region or not.

As for the high-density region, we filter the intensity noises and obtain the point p's denoised intensity, $I_f(p)$, as follows:

$$I_f(p) = \underset{I(q), q \in \boldsymbol{N}_p}{\text{argmin}}\{\Delta I_{sum_q}\} = \underset{I(q), q \in \boldsymbol{N}_p}{\text{argmin}}\{\sum_{q^{'} \in \boldsymbol{N}_p, q \neq q^{'}} |I(q) - I(q^{'})|\} \tag{10}$$

where $I(q)$ represents the point q's intensity value. $\boldsymbol{N}_p$ represent the 3D point p's neighboring points which can be obtained by KDTree algorithm. ΔI_{sum_q} computes the sum of intensity difference between point q and the points in $\boldsymbol{N}_p$. The Eq. (10) implies that the point p's intensity should consider its contextual intensities.

As for the low-density region, we use a bilateral filter (Elad, 2002) to remove the intensity noises and obtain the point p's denoised intensity,

Table 1
Description of the datasets used in the experiments.

Datasets	MLS systems	Location	Density (pts/m^2)	Length (km)	Number of Points
Datasets I	Chchav Alpha3D	Hangzhou, China	110	1.24	9,259,200
Datasets II	Trimble	Beijing, China	253	0.7	20,504,300
Datasets III	RIEGL VMX-450	Fuzhou, China	297	0.46	41,590,228
Datasets IV	Lynx Mobile Mapper	Hengyang, China	162	1.27	17,205,416

Table 2
Parameter description.

Parameter name	Description	Value
t_0	Minimum transmittance	0.1
M	Intensity intervals	10
$th_c r_d$	The threshold for distinguishing high-density areas from low-density areasA searching radius to find neighboring points	95 cm

Table 3
The average time of our proposed method on processing a road section (Units: Seconds).

Datasets	Preprocessing	Intensity correction	Intensity transformation	Intensity denoising	Total
Datasets I	38.73	0.82	0.11	25.44	65.10
Datasets II	41.51	0.09	0.04	5.62	47.26
Datasets III	32.81	0.57	0.09	25.08	58.55
Datasets IV	10.19	0.08	0.02	3.40	13.69

$I_f(p)$, as follows:

$$I_f(p) = \frac{1}{W_p}\sum_{q\in N_p} G_{\sigma_d}(p,q)G_{\sigma_I}(I_t(p),I_t(q))I_t(q) \tag{11}$$

$$G_{\sigma_d}(p,q) = exp\left(-\frac{\|p-q\|_2^2}{2{\sigma_d}^2}\right) \tag{12}$$

$$G_{\sigma_I}(I_t(p),I_t(q)) = \exp\left(-\frac{|I_t(p)-I_t(q)|^2}{2{\sigma_I}^2}\right) \tag{13}$$

where the function $G_{\sigma_d}(\bullet)$ and $G_{\sigma_I}(\bullet)$ compute the weights of spatial distance and intensity difference, respectively. σ_d and σ_I are the standard deviations of spatial distance and intensity difference in the low-density region, respectively. $I_t(p)$ is the transformed intensity of the 3D point p. N_p is the 3D point p's neighboring points which can be obtained by KDTree algorithm. W_p is a normalization term which is calculated as follows:

$$W_p = \sum_{q\in N_p} G_{\sigma_d}(p,q)G_{\sigma_I}(I_t(p),I_t(q)) \tag{12}$$

After applying the bilateral filter, the intensities in low-density regions will be smooth for the on-road objects, i.e. marking lines (see Fig. 5 (b)).

Table 4
Signal-Noise Ratio (SNR) before and after applying the proposed intensity transformation on datasets I-IV.

	Datasets I	Datasets II	Datasets III	Datasets IV
Original point clouds	6.64	5.00	5.05	0.95
Point clouds after intensity transformation	29.00	14.30	42.70	24.85

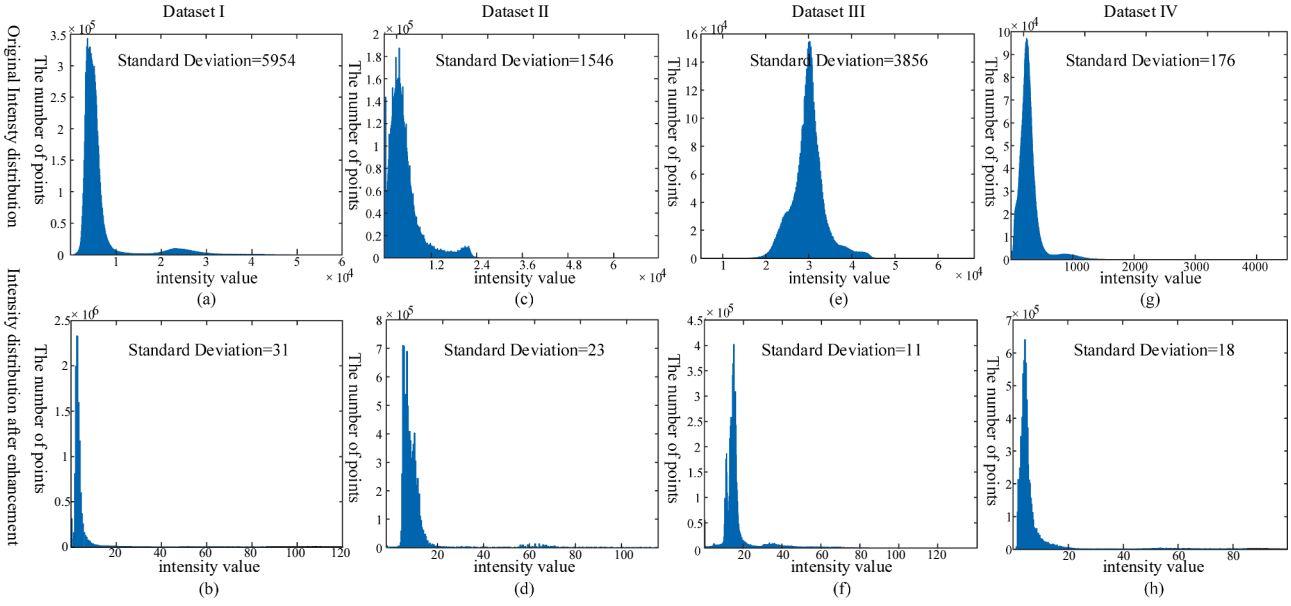

Fig. 6. The standard deviation of intensity before and after applying our proposed method on Dataset I-IV. Specifically, (a), (c), (e) and (g) are the intensity distribution and standard deviation of intensity in the original point clouds. (b), (d), (f) and (h) are the intensity distribution and standard deviation of intensity after applying our proposed method.

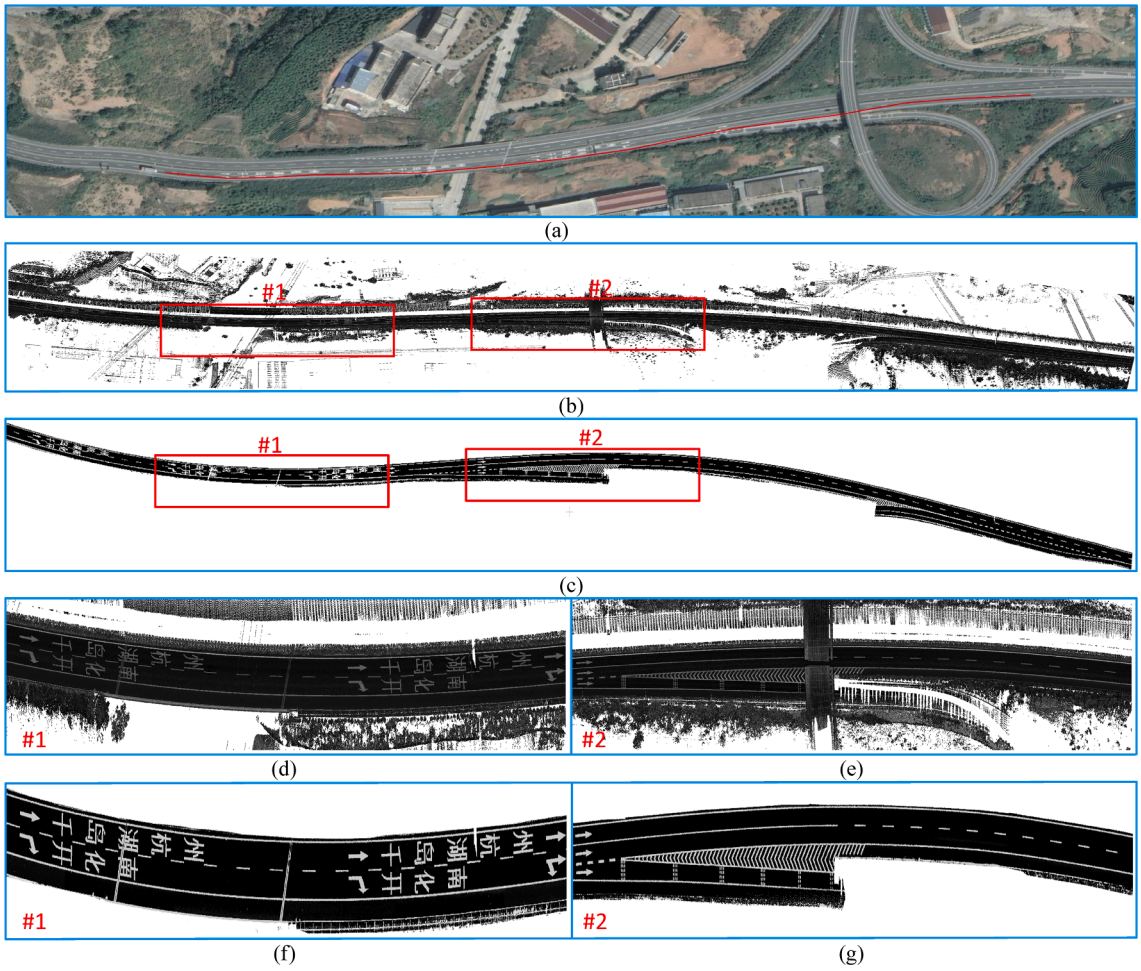

Fig. 7. Intensity enhancement results of our proposed method on a part of Dataset I. Specifically, (a) high-resolution image of the data location, (b) original MLS point clouds. (c) intensity-enhanced point clouds, (d) close-up views of region #1in (b), (e) close-up views of region #2 in (b), (e) close-up views of region in (c), and (g) close-up views of region #2 in (c).

4. Experiments

4.1. Study area and dataset

In order to verify the capabilities of our proposed method on enhancing intensity in different MLS point-cloud scenarios, we conduct the qualitative and quantitative experiments on four different datasets, i.e. Datasets I-IV. The used datasets contain different road scenarios covering most road conditions. Specifically, point clouds in Dataset I are acquired at the highway in Hangzhou city, China, by equipping a minivan with the Chchav Alpha3D MLS system. The length of the acquired point-cloud road is about 1.24 km, and some sections of its road surface and road marking are severely worn. Point clouds in Dataset II are obtained at a suburban road located in Beijing city, China, by using the Trimble MLS system. The length of the obtained point-cloud is about 0.7 km. In the suburban road, the occlusions and road wear occur frequently, which causes the incomplete and damaged point-cloud road. Dataset III contains the point clouds collected at urban roads in Fuzhou city, China, by using RIEGL VMX-450 equipped with two VQ-450 laser scanners. The collected point clouds contain different and complex road conditions such as severe occlusion caused by road congestion, road abrasion, water stains on the road, etc. For Dataset IV, the point clouds are captured at the city road in Hengyang city, China, by a Lynx Mobile Mapper MLS system. The captured point clouds, whose length is approximate 1.27 km, have many different types of road markings. Additionally, the captured intensities are severely influenced by the scanning distances. More detailed information on the used datasets is provided in Table 1.

4.2. Implemental details

In this subsection, we detail the experimental settings of each step in our proposed intensity-enhanced method in Table 2. At the data preprocessing step, we partition the captured point clouds into consecutive road sections with a length of about 25 m. Here, the length of the road section is experientially set for obtaining a proper processing efficiency according to our used hardware. At the intensity correction step, we use a cubic polynomial function to fit the point-cloud data of the road surface with the consistent intensity. At the intensity transformation step, we experientially set t_0 to be 0.1. In addition, the number of intensity intervals, $\boldsymbol{M}$, is set to be 10. At the intensity denoising step, we set the threshold th_c to be 9 for distinguishing whether a 3D point belongs to a high-density region or low-density region. The density of the 3D point is defined by calculating the neighboring points within a searching radius r_d. Here, we set r_d to be 5 cm.

In the paper, all experiments were coded with MATLAB R2020b under the Window 11 operating system, and performed on an HP workstation with eight Intel core i7 processors of 2.9 GHz and a RAM of 32 GB. The execution time of our proposed method on processing a road section was reported in Table 3. As shown in Table 3, our proposed method on accomplishing the intensity enhancement for a road section of 25 m takes approximately one minute. Most of the time is spent on the

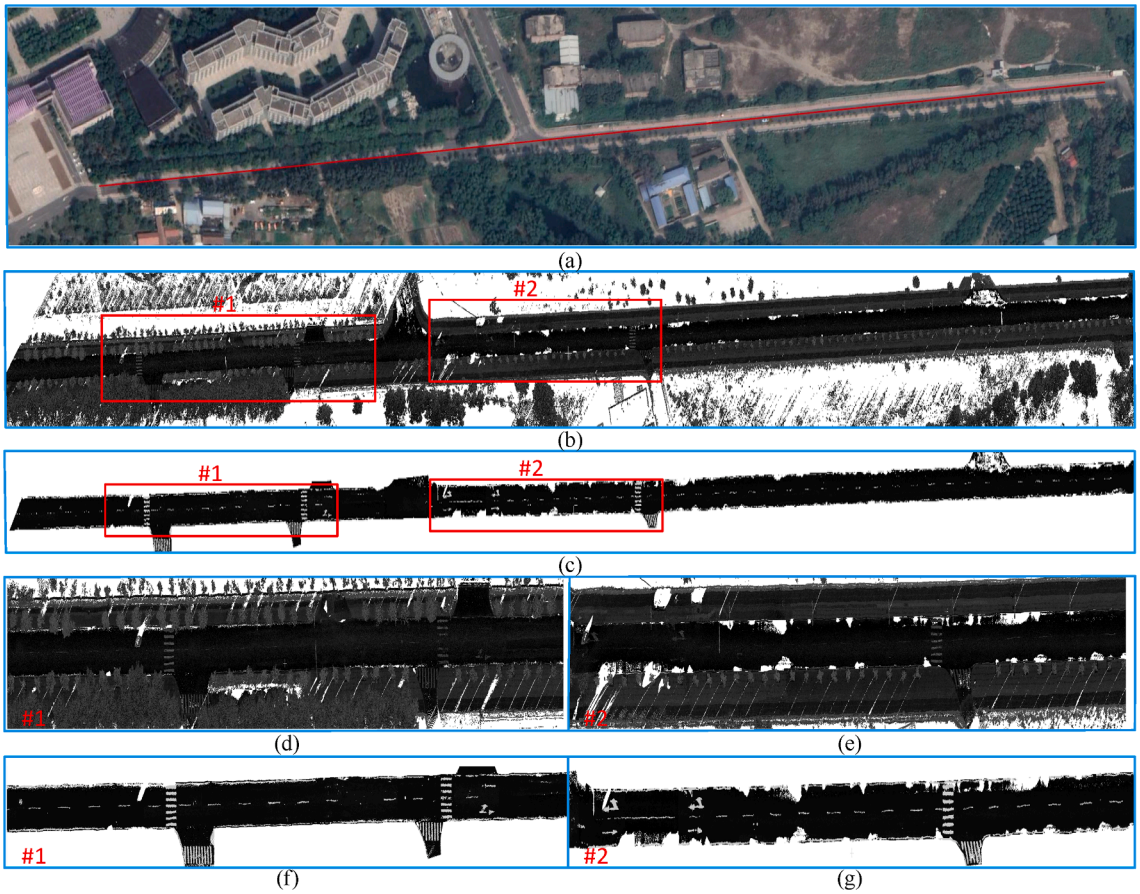

Fig. 8. Intensity enhancement results of our proposed method on a part of Dataset II. Specifically, (a) high-resolution image of the data location, (b) original MLS point clouds. (c) intensity-enhanced point clouds, (d) close-up views of region #1in (b), (e) close-up views of region #2 in (b), (f) close-up views of region in (c), and (g) close-up views of region #2 in (c).

steps of data preprocessing and intensity denoising. We believe that the processing time of our proposed method is acceptable for many intensity-based applications.

4.3. Experimental results

In the experiments, both qualitative and quantitative evaluations are performed on Datasets I-IV for demonstrating the effectiveness of our proposed method. For the quantitative evaluation, we draw the curves where the number of points varies with the intensity values, and calculated the standard deviation of the intensity values of all the points in each dataset. As shown in Fig. 6, the standard deviations of the intensity values on Dataset I-IV sharply decrease from (5954, 1546, 3856, 176) to (31, 23, 11, 18), respectively. This demonstrates that our proposed method can effectively eliminate the intensity noise and the intensity inconsistency. Moreover, the curves in Fig. 6 (a), (c), (e) and (g) illustrate that the points are scattered at different intensity values because of intensity noise and intensity inconsistency. In contrast, the curves in Fig. 6 (b), (d), (f) and (h) demonstrate that the points are concentrated in a small range of intensity values. This further exhibits that our proposed method can achieve the intensity enhancement by implementing intensity noise elimination and intensity inconsistency correction in MLS point clouds.

Moreover, the Signal-Noise Ratio (SNR) is introduced to quantitatively analyze the performance of our proposed method. The SNR of a point cloud scenes is calculated by

$$SNR = 10^{*}log\frac{\sum_{i=1}^{N}(I_o^i)^2}{\sum_{i=1}^{N}(I_o^i - I_t^i)^2} \tag{13}$$

where N represents the number of points in the point cloud scene.I_o^i and I_t^i are the intensity value of point p_i in the input point clouds and the point clouds with no intensity noises, respectively. Here, we treated the final intensity-enhanced point clouds obtained by our proposed method as the point clouds with no intensity noises. Table 4 records the SNR before and after applying the intensity transformation on datasets I-IV. As shown in Table 4, we can see that the intensity transformation can largely increase the SNR values, which demonstrates the effectiveness of the dark channel prior in the proposed method.

For the qualitative evaluation, we provide Figs. 7–10 to exhibit the intensity enhancement results of our proposed method on Dataset I-IV, respectively. To better show the experimental results of our proposed method in the top view, we only present the intensity-enhanced point clouds with road surface. Here, we use the grayscale information to represent the intensity value, where the darker color indicates the smaller intensity value. As exhibited in Figs. 7–10, the contrast in original point cloud scenes is much lower than intensity-enhanced point-cloud scenes, which indicates that the intensity correction and intensity transformation proposed in our intensity-enhanced method can perform well in improving the intensity quality in different road scenarios. In addition, the intensity values in the intensity-enhanced point-cloud scenes are much smoother than original point-cloud scenes, which reflects that our proposed method is able to deal with the intensity noise in different road scenarios.

To further demonstrate the correctness of our proposed method, we provide the intensity-enhanced results on the scanning lines. Fig. 11 demonstrates the comparison of the intensity distribution of the scanning lines before and after applying our proposed method. The intensity-

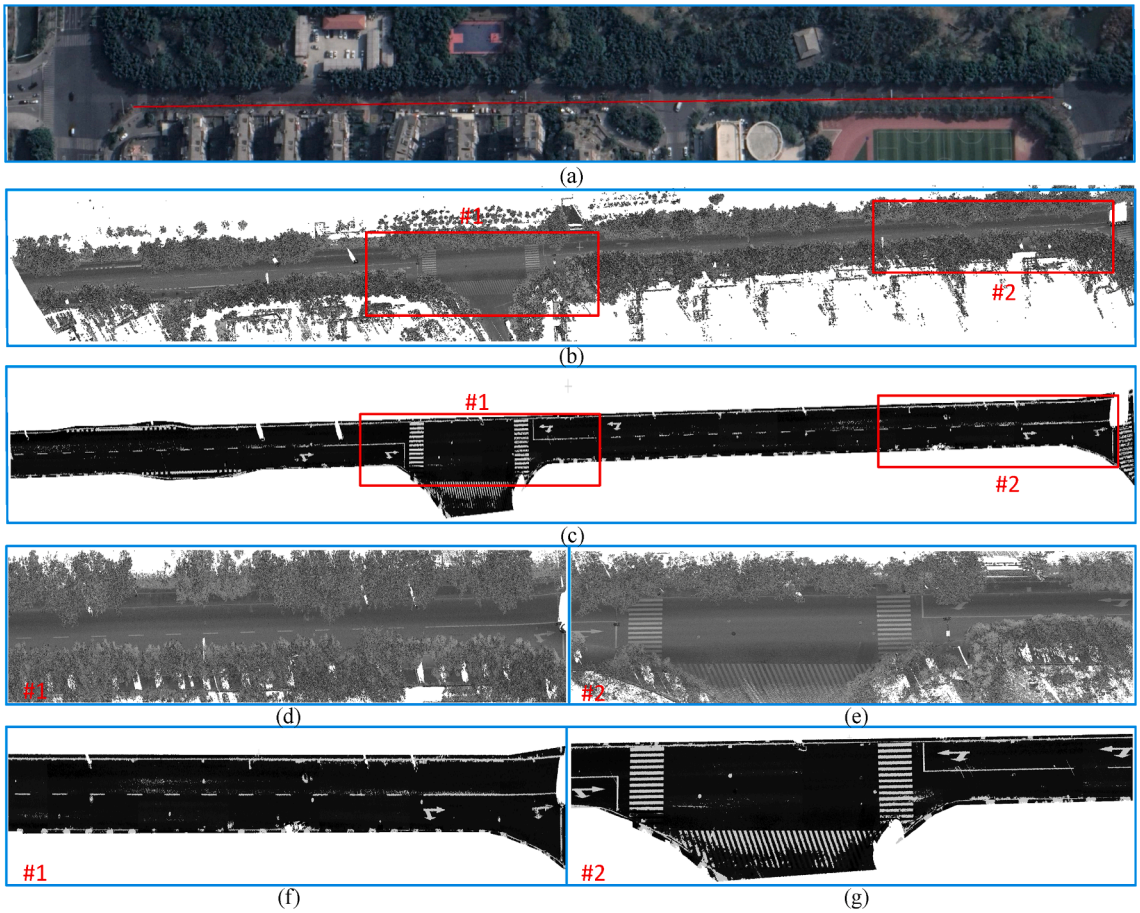

Fig. 9. Intensity enhancement results of our proposed method on a part of Dataset III. Specifically, (a) high-resolution image of the data location, (b) original MLS point clouds. (c) intensity-enhanced point clouds, (d) close-up views of region #1in (b), (e) close-up views of region #2 in (b), (f) close-up views of region in (c), and (g) close-up views of region #2 in (c).

enhanced effect in Fig. 11 can be commonly observed in the results obtained by our proposed method. As shown in Fig. 11, the intensity distributions of the intensity-enhanced scanning lines are much smoother than those of the original scanning lines. Additionally, the intensities of the points in the scanning lines are centrally distributed around several intensity values. The observations indicate that our proposed method can effectively accomplish the task of intensity enhancement in MLS point clouds.

4.4. Discussion

To discuss the effects of each component in our proposed method on the intensity enhancement, we conducted the ablation experiments on Datasets I-IV. We compared our proposed method with six different methods, i.e., IC method, IT method, ID method, IC + IT method, IC + ID method, and IT + ID method. Specifically, Intensity Correction (IC) method only executes the intensity correction based on scanning distance. Intensity Transformation (IT) method only implements the intensity transformation by applying the dark channel prior. Intensity Denoising (ID) method only conducts the intensity denoising approach introduced in Section 3.4. The IC + ID method combines the IC method with the ID method. The IC + IT method combines the IC method with the ID method. The IT + ID method integrates the IT method with the ID method. Fig. 12 exhibits the comparative results of different methods on intensity enhancement at five different point cloud scenarios. As shown in Fig. 12, the road abrasion exists in the scenes 1, 2 and 3. Moreover, there is a water body in scene 5 because of the rainy day. The road abrasion and water body causes the intensity noises in the obtained point clouds. After applying the IC method, the intensities of the points belonging to the same category remain consistent. The intensity contrast of the points with different intensities gets enhanced after applying the IT method. In addition, isolated intensity noises are removed after applying the ID method. The results of the IT, IC, and ID methods demonstrate that intensity correction, intensity transformation, and intensity denoising play different roles in intensity enhancement of MLS point clouds.

To analyze the impact of intensity interval $\boldsymbol{M}$ on the results of intensity transformation, we have implemented the proposed method at the following configurations: 5, 10, 15 and 20. Fig. 4 presents the results of intensity transformation on the different configurations of intensity interval $\boldsymbol{M}$. As shown in Fig. 13, when the intensity interval $\boldsymbol{M}$ is set to 5, 15 and 20, the road markings are not clear and many intensity values of the road markings are inaccurately transformed. When the intensity interval $\boldsymbol{M}$ is set to 10, most of the intensity values of road makings are correctly transformed and the intensity contrast can be used to accurately distinguish the points belonging to road markings or not. Therefore, we set the value $\boldsymbol{M}$ at 10 in the experiments.

Although our proposed method can achieve a satisfactory performance on the task of intensity enhancement in MLS point clouds, there are still some failure cases in the complex scenarios. These failure cases are shown in Fig. 14. Concretely, in the first failure case, when the manhole cover is too small, it may be treated as intensity noise, which may be eliminated at the intensity denoising step. In the second failure case, when the relectance of the road surface is similar to that of the heavily-worn road markings, the intensity transformation may fail to recover and enhance the intensities of the road markings. In the third

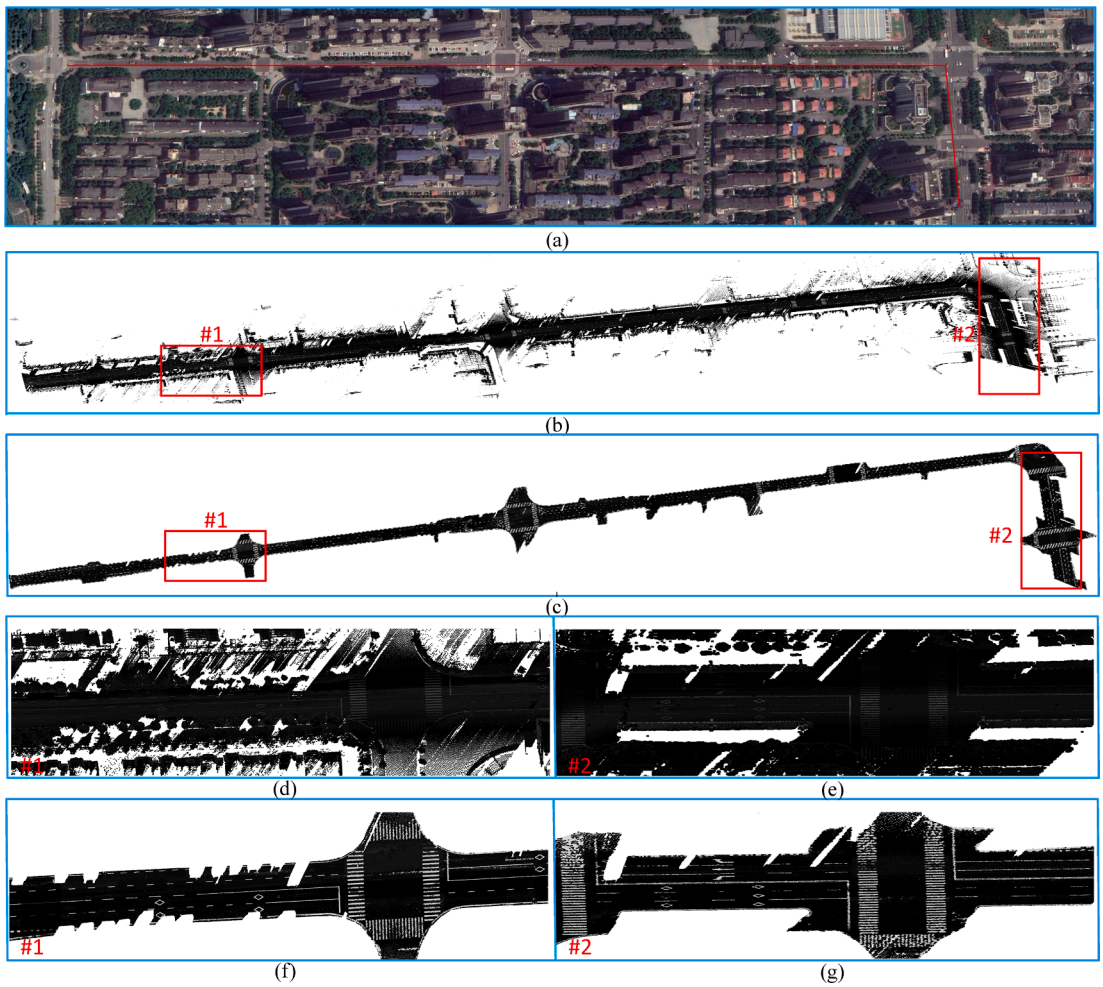

Fig. 10. Intensity enhancement results of our proposed method on a part of Dataset IV. Specifically, (a) high resolution image of the data location, (b) original MLS point clouds. (c) intensity-enhanced point clouds, (d) close-up views of region #1in (b), (e) close-up views of region #2 in (b), (f) close-up views of region in (c), and (g) close-up views of region #2 in (c).

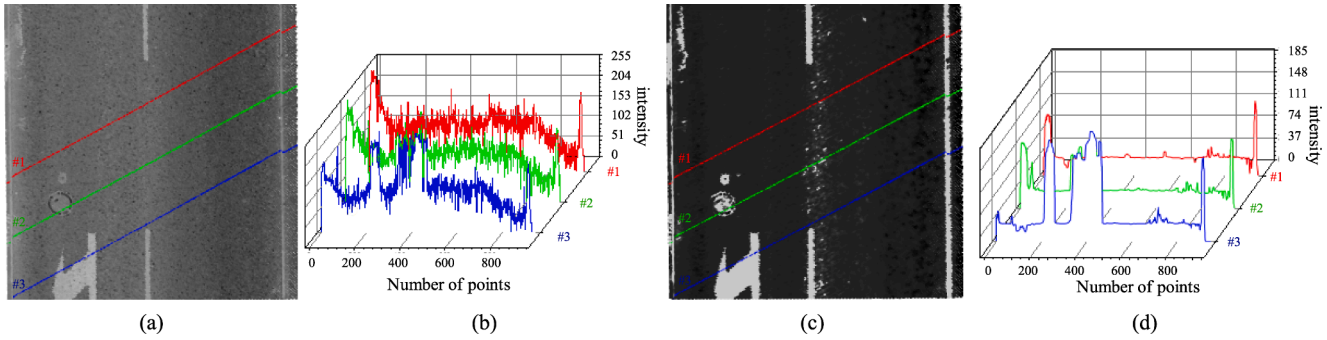

Fig. 11. Intensity distributions in the scanning lines: (a) the scan lines in the original point clouds; (b) intensity distributions in the scanning lines of original point clouds; (c) the scan lines in the intensity-enhanced point clouds; (d) intensity distributions in the scanning lines of the intensity-enhanced point clouds.

failure case, the intensities of the heavily-worn road markings may sometimes be over-enhanced. Despite these failure cases, our proposed method can still perform well on executing the intensity enhancement in the heavily worn road scenarios.

5. Conclusions

To effectively enhance the intensities in MLS point clouds for various intensity-based applications, this paper proposes a novel method composed of three components, i.e. intensity correction based on scanning distance, intensity transformation based on dark channel prior, and intensity denoising via multi-filter integration. Particularly, to remove the pepper-and-salt noise caused by the road abrasion, the dark channel prior is introduced and adapted to transform the intensities for effectively enhancing the intensity contrast among the points with different intensities. Evaluations have been conducted on four datasets where point clouds are collected by different MLS systems at different road scenarios. The qualitative results have exhibited that the proposed

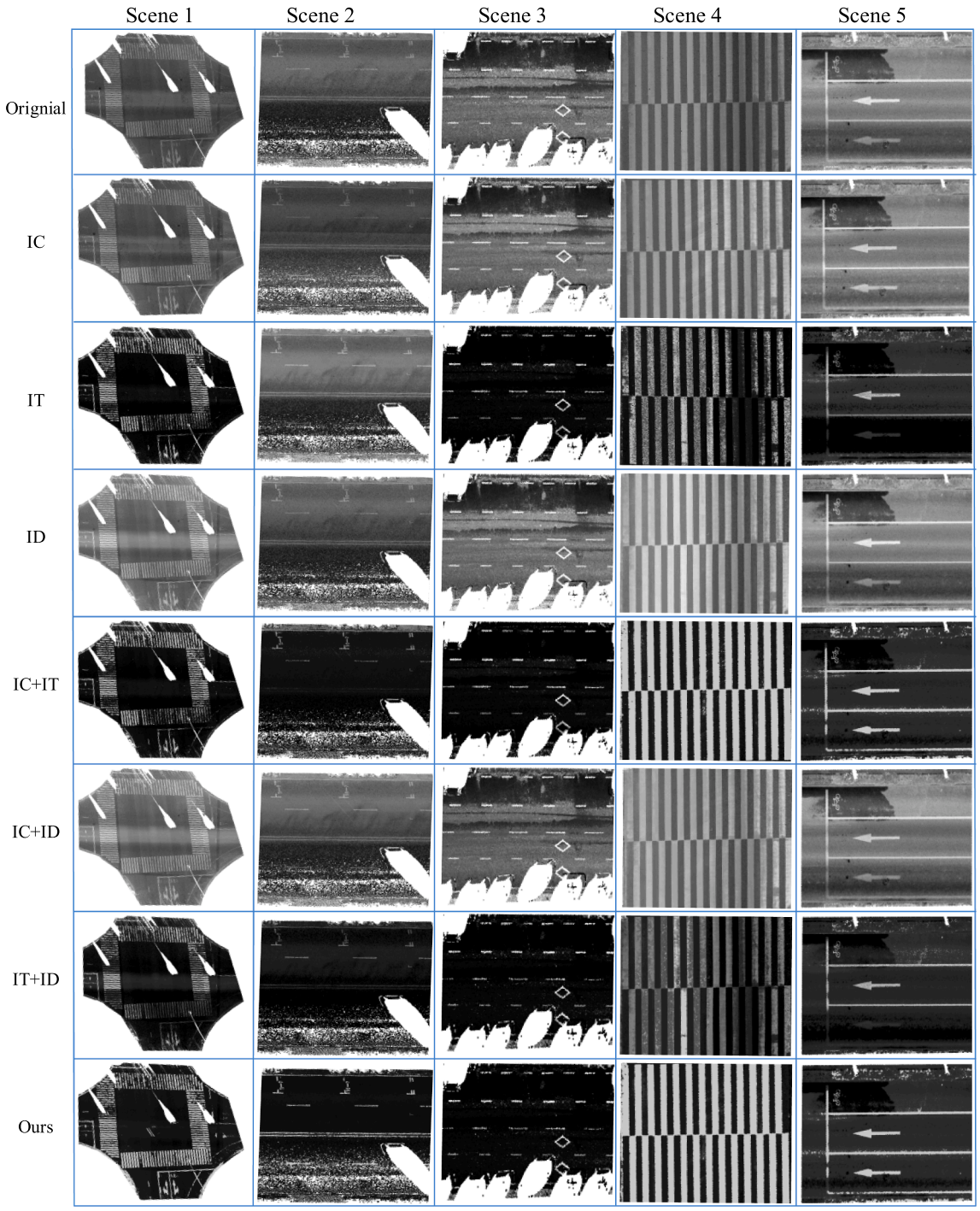

Fig. 12. Comparisons of different methods on intensity enhancement at five different point cloud scenarios.

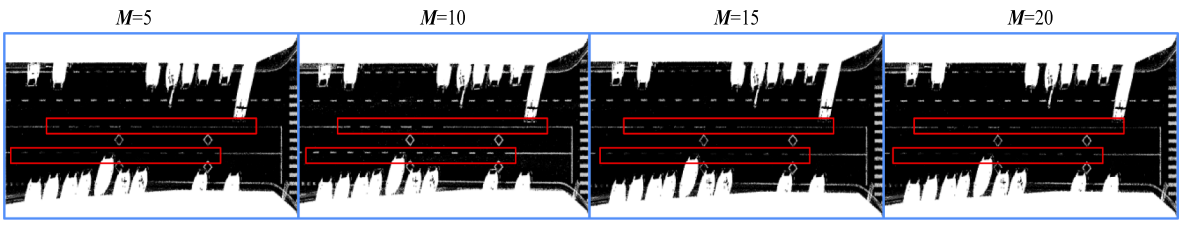

Fig. 13. The impact of different ***M*** values used in our proposed method on intensity transformation. Here, the red rectangle emphasizes the intensity variations in different configurations.

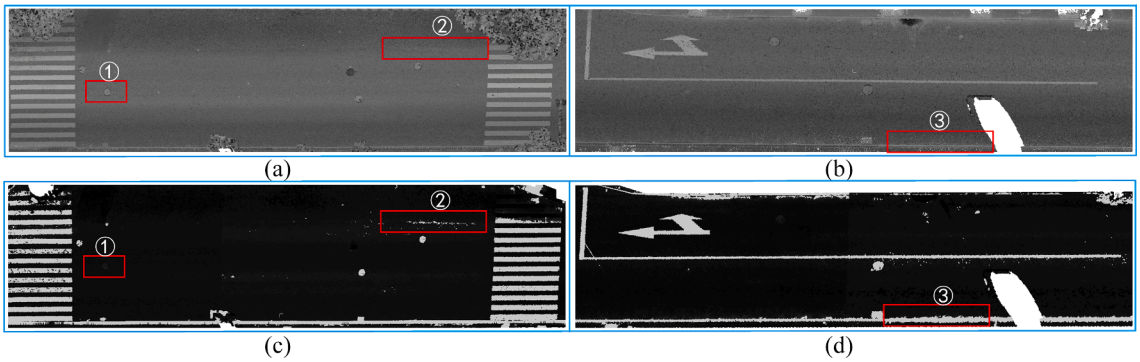

Fig. 14. Some failure cases in our proposed method on enhancing the intensities of point cloud scenes.

method can largely reduce the standard deviations of the intensities from (5954, 1546, 3856, 176) to (31, 23, 11, 18) for Dataset I-IV, respectively. This reflects the remarkable performance of our proposed method on intensity enhancement. In addition, the quantitative results have further demonstrated that our proposed can achieve the task of intensity enhancement in various road scenarios.

Funding

This study was financially supported by National Natural Science Foundation of China (Grant No. 61801121, No. 42071446, No. 41871380, No. U1705262), Natural Science Foundation of Fujian Province (No. 2019J05034, No. 2018J07005), Fujian Foreign Cooperation Project Foundation (No. 2020I0007).

CRediT authorship contribution statement

Lina Fang: Validation, Formal analysis, Investigation, Resources, Visualization, Supervision, Funding acquisition. **Hao Chen:** Conceptualization, Software, Methodology, Writing – original draft, Validation. **Huan Luo:** Conceptualization, Software, Methodology, Writing – original draft, Writing – review & editing, Funding acquisition. **Yingya Guo:** Conceptualization, Methodology, Writing – original draft, Writing – review & editing. **Jonathon Li:** Validation, Resources, Supervision.

Declaration of Competing Interest

The authors declare that they have no known competing financial interests or personal relationships that could have appeared to influence the work reported in this paper.

References

Anttila, K., Hakala, T., Kaasalainen, S., Kaartinen, H., Nevalainen, O., Krooks, A., Kukko, A., Jaakkola, A., 2016. Calibrating laser scanner data from snow surfaces: Correction of intensity effects. Cold Reg. Sci. Technol. 121, 52–59.

Al-Shayea, T.K., Mavromoustakis, C.X., Batalla, J.M., Mastorakis, G., Mukherjee, M., Pallis, E., 2020. A novel gaussian in denoising medical images with different wavelets for internet of things devices. In: GLOBECOM 2020 – 2020 IEEE Global Communications Conference, pp. 1–6.

Cheng, M., Zhang, H., Wang, C., Li, J., 2017. Extraction and classification of road markings using mobile laser scanning point clouds. IEEE J. Sel. Top. Appl. Earth Obs. Remote Sens. 10 (3), 1182–1196.

Cheng, X., Mao, J., Li, J., Zhao, H.u., Zhou, C., Gong, X., Rao, Z., 2021. An EEMD-SVD-LWT algorithm for denoising a lidar signal. Measurement 168, 108405. https://doi.org/10.1016/j.measurement.2020.108405.

Dias, P., Sequeira, V., Gonçalves, J., Vaz, F.J.R., Systems, A., 2002. Automatic registration of laser reflectance and colour intensity images for 3D reconstruction. Rob. Auton. Syst. 39, 157–168.

Ding, Q., Chen, W.u., King, B., Liu, Y., Liu, G., 2013. Combination of overlap-driven adjustment and Phong model for LiDAR intensity correction. ISPRS J. Photogramm. Remote Sens. 75, 40–47.

Fang, W., Husng, X., Zhang, F., Li, D., 2015. Intensity correction of terrestrial laser scanning data by estimating laser transmission function. IEEE Trans. Geosci. Remote Sens. 53 (2), 942–951.

Fang, L., Shen, G., Luo, H., Chen, C., Zhao, Z., 2021. Automatic extraction of roadside traffic facilities from mobile laser scanning point clouds based on deep belief network. IEEE Trans. Intell. Transp. Syst. 22 (4), 1964–1980.

Guan, H., Li, J., Yu, Y., Wang, C., Chapman, M., Yang, B., 2014. Using mobile laser scanning data for automated extraction of road markings. ISPRS J. Photogramm. Remote Sens. 87, 93–107.

Höfle, B., Pfeifer, N., 2007. Correction of laser scanning intensity data: Data and model-driven approaches. ISPRS J. Photogramm. Remote Sens. 62 (6), 415–433.

He, K., Sun, J., Tang, X., 2010. Single image haze removal using dark channel prior. IEEE Trans. Pattern Anal. Mach. Intell. 33 (12), 2341–2353.

Huang, P., Cheng, M., Chen, Y., Luo, H., Wang, C., Li, J., 2017. Traffic sign occlusion detection using mobile laser scanning point clouds. IEEE Trans. Intell. Transp. Syst. 18 (9), 2364–2376.

Li, Y., Hua, L., Li, J., et al., 2016. Scan line based road marking extraction from mobile LiDAR point clouds. Sensors 56 (7), 3631–3644.

Li, Y., Ma, L., Zhong, Z., Liu, F., Chapman, M.A., Cao, D., Li, J., 2021. Deep learning for LiDAR point clouds in autonomous driving: A review. IEEE Trans. Neural Networks Learn. Syst. 32 (8), 3412–3432.

Luo, H., Wang, C., Wen, C., Chen, Z., Zai, D., Yu, Y., Li, J., 2018. Semantic labeling of mobile LiDAR point clouds via active learning and higher order MRF. IEEE Trans. Geosci. Remote Sens. 56 (7), 3631–3644.

Luo, H., Wang, C., Wen, Y., Guo, W., 2019. 3-D Object classification in heterogeneous point clouds via bag-of-words and joint distribution adaption. IEEE Geosci. Remote. Sens. 16 (12), 1909–1913. https://doi.org/10.1109/LGRS.2019.2911200.

Luo, H., Zheng, Q., Fang, L., Guo, Y., Guo, W., Wang, C., Li, J., 2021. Boundary-Aware graph Markov neural network for semiautomated object segmentation from point clouds. Int. J. Appl. Earth Obs. Geoinf. 104, 102564. https://doi.org/10.1016/j.jag.2021.102564.

Elad, M., 2002. On the origin of the bilateral filter and ways to improve it. IEEE Trans. Image Process. 11 (10), 1141–1151.

Mahmoudabadi, H., Olsen, M.J., Todorovic, S., 2016. Efficient terrestrial laser scan segmentation exploiting data structure. ISPRS J. Photogramm. Remote Sens. 119, 135–150.

Ma, L., Li, Y., Li, J., Yu, Y., Junior, J.M., Goncalves, W.N., Chapman, M.A., 2021. Capsule-based networks for road marking extraction and classification from mobile LiDAR point clouds. IEEE Trans. Intell. Transp. Syst. 22 (4), 1981–1995.

Mi, X., Yang, B., Dong, Z., Liu, C., Zong, Z., Yuan, Z., 2021. A two-stage approach for road marking extraction and modeling using MLS point clouds. ISPRS J. Photogramm. Remote Sens. 180, 255–268.

Pan, Y., Yang, B., Li, S., Yang, H., Dong, Z., Yang, X., 2019. Automatic road markings extraction, classification and vectorization from mobile laser scanning data. ISPRS Geospatial Week 2019, 1089–1096.

Rastiveis, H., Shams, A., Sarasua, W.A., Li, J., 2020. Automated extraction of lane markings from mobile LiDAR point clouds based on fuzzy inference. ISPRS J. Photogramm. Remote Sens. 160, 149–166.

Schmitz, B., Holst, C., Medic, T., Lichti, D., Kuhlmann, H., 2019. How to efficiently determine the range precision of 3D terrestrial laser scanners. Sensors 19 (6), 1466. https://doi.org/10.3390/s19061466.

Song, Y., Li, H., Zhai, G., He, Y., Bian, S., Zhou, W., 2021. Comparison of multichannel signal deconvolution algorithms in airborne LiDAR bathymetry based on wavelet transform. Sci. Rep. 11, 16988.

Thundathil, R., Schwitalla, T., Behrendt, A., Wulfmeyer, V., 2021. Impact of assimilating lidar water vapour and temperature profiles with a hybrid ensemble transform Kalman filter: Three-dimensional variational analysis on the convection-permitting scale. Q. J. R. Meteorolog. Soc. 147 (741), 4163–4185.

Teo, T.A., Yu, H.L., 2015. Empirical radiometric normalization of road points from terrestrial mobile lidar system. Remote Sens. 7 (5), 6336–6357.

Tan, K., Cheng, X., 2016. Correction of incidence angle and distance effects on TLS intensity data based on reference targets. Remote Sens. 8 (3), 251.

Wen, C., Sun, X., Li, J., Wang, C., Guo, Y., Habib, A., 2019. A deep learning framework for road marking extraction, classification and completion from mobile laser scanning point clouds. ISPRS J. Photogramm. Remote Sens. 147, 178–192.

Wu, Q., Zhong, R., Dong, P., Mo, Y., Jin, Y., 2021. Airborne lidar intensity correction based on a new method for incidence angle correction for improving land-cover classification. Remote Sens. 13 (3), 511. https://doi.org/10.3390/rs13030511.

Wang, Z., Xia, Q., Du, J., Huang, S., Su, J., Junior, J.M., Li, J., Cai, G., 2021. 3D MSSD: A multilayer spatial structure 3D object detection network for mobile LiDAR point clouds. Int. J. Appl. Earth Obs. Geoinf. 102, 102406. https://doi.org/10.1016/j.jag.2021.102406.

Yang, B., Fang, L., Li, Q., Li, J., 2012. Automated extraction of road markings from mobile lidar point clouds. Photogramm. Eng. Remote Sens. 78 (4), 331–338.

Yang, B., Fang, L., Li, J., 2013. Semi-automated extraction and delineation of 3D roads of street scene from mobile laser scanning point clouds. ISPRS J. Photogramm. Remote Sens. 79, 80–93.

Yang, B., Liu, Y., Dong, Z., Liang, F., Li, B., Peng, X., 2017. 3D local feature bkd to extract road information from mobile laser scanning point clouds. ISPRS J. Photogramm. Remote Sens. 130, 329–343.

Yan, L.i., Liu, H., Tan, J., Li, Z., Xie, H., Chen, C., 2016. Scan line based road marking extraction from mobile lidar point clouds. Sensors 16 (6), 903. https://doi.org/10.3390/s16060903.

Yu, Y., Guan, H., Li, D., Jin, C., Wang, C., Li, J., 2020. Road manhole cover delineation using mobile laser scanning point cloud data. IEEE Geosci. Remote Sens. Lett. 17 (1), 152–156.

Ye, C., Zhao, H., Ma, L., Jiang, H., Li, H., Wang, R., Chapman, M., Marcato, J., Li, J., 2021. Robust lane extraction from MLS point clouds towards HD maps especially in curve roads. IEEE Trans. Intell. Transp. Syst. 1–14.

Zhang, L., Chang, J., Li, H., Liu, Z.X., Zhang, S., Mao, R., 2020. Noise reduction of lidar signal via local mean decomposition combined with improved thresholding method. IEEE Access 8, 113943–113952.